Results in Engineering 32 (2026) 112573

Contents lists available at ScienceDirect

Results in Engineering

journal homepage: www.sciencedirect.com/journal/results-in-engineering

Research paper

Early-age mechanical performance of cement mortars incorporating treated wood ash

Oskars Lescinskis [a,*], Girts Bumanis [a], Genadijs Sahmenko [a], Tatjana Tambovceva [b], Danute Vaiciukyniene [c], Sakdirat Kaewunruen [d], Diana Bajare [a]

[a] Institute of Sustainable Building Materials and Engineering Systems, Faculty of Civil and Mechanical Engineering, Riga Technical University, 6A Kipsalas, LV-1048 Riga, Latvia
[b] Governance and Security Institute, Faculty of Engineering Economics and Management, Riga Technical University, LV-1048 Riga, Latvia
[c] Building Materials and Structures Research Centre, Faculty of Civil Engineering and Architecture, Kaunas University of Technology, Studentu st. 48, Kaunas LT-51367, Lithuania
[d] Department of Civil Engineering, School of Engineering, University of Birmingham, Birmingham, B15 2TT, United Kingdom

ARTICLE INFO

Keywords:
Wood ash
Portland cement
Partial cement replacement
Cement mortar
Compressive strength

ABSTRACT

Wood ash (WA), a by-product of biomass combustion, is generated in large quantities, yet its utilization as partial replacement of Portland cement (PC) remains limited due to variability in its properties and performance. This study investigates the early-age mechanical performance of treated WA as a 20% partial replacement of PC in cement mortars. Four types of WA (fly ash, two bottom ash fractions, and a slag fraction) were subjected to five sequential treatment routes comprising ball-milling alone, ball-milling followed by water-washing, ball-milling followed by slaking, ball-milling followed by calcination, and ball-milling followed by water-washing and calcination. Compressive strength was measured at 2, 7, and 28 days, and a Strength Activity Index (SAI) was calculated from the compressive strength results to compare the mechanical performance of WA-containing mortars. The 75% SAI value specified in ASTM C618 was used as a comparative benchmark, and none of the investigated WA mortar mixtures reached this reference value after 28 days of curing. The best-performing mixtures were bottom ash-based mortars, with SAI values reaching 65–71% at 28 days. In contrast, ball-milled fly ash-based mixtures showed the lowest performance, with early-age compressive strength as low as 4.1 MPa at 2 days. Overall, the findings indicate limited early-age mechanical performance at a 20% cement replacement level. The study provides comparative experimental data on the influence of different treatment methods on the early-age mechanical performance of WA.

1. Introduction

The concept of the circular economy has gained momentum as a strategic framework for mitigating environmental and resource challenges posed by the linear "take-make-dispose" model dominant in industrial and construction activities [1].

In the built environment, strategies focus on reducing raw material extraction, utilizing waste streams, and extending product life cycles through reuse and recycling. The construction sector is a major consumer of resources and contributor to waste generation, and Portland cement (PC), the primary binder in concrete, is a focal point for decarbonization due to its high raw material demand and energy-intensive production process [2,3]. Cement manufacture releases approximately 900 kg of CO_2 per ton of PC produced, with the industry accounting for an estimated 7–8% of global anthropogenic CO_2 emissions [4,5], in addition to substantial consumption of limestone, clay, and fossil fuels.

The urgent need for sustainable construction practices has led to extensive research into the use of industrial and agricultural by-products in cement-based systems. These waste-derived materials are commonly explored as partial cement replacement materials aimed at reducing clinker consumption and promoting resource efficiency. Wood ash (WA), a residue from biomass combustion, has been investigated within this context due to its variable chemical composition, which may include CaO, $Ca(OH)_2$, $CaCO_3$, and calcium silicates, suggesting potential interaction with cementitious systems [6]. The high annual production of WA—estimated at 18.5 million tons globally, including 2.42

* Corresponding author.
E-mail address: oskars.lescinskis_1@rtu.lv (O. Lescinskis).

https://doi.org/10.1016/j.rineng.2026.112573
Received 31 March 2026; Received in revised form 14 August 2026; Accepted 20 August 2026
Available online 21 August 2026

million tons in Europe—underscores its availability as a widely distributed secondary material stream [7]. Approaches involving waste-derived materials aim to reduce resource consumption and divert industrial by-products from disposal [3,8].

However, the performance of WA in cement-based systems strongly depends on its physico-chemical characteristics, which vary with feedstock and combustion conditions [9,10]. Undesirable constituents such as unburned carbon and soluble salts can negatively affect mortar and concrete properties, including workability, setting time, and strength development [7,8,11]. To address these challenges, various treatment methods—including ball-milling, water-washing, slaking, and calcination—have been explored to improve WA quality. Ball-milling can reduce particle size, increase specific surface area, and induce structural disorder, which may enhance its reactivity and packing behavior [12], whereas water-washing removes detrimental soluble components [11], slaking can pre-hydrate reactive CaO and reduce potential swelling associated with its subsequent hydration [13], and calcination can modify WA characteristics and reactivity [14]. Combined approaches have also shown promise in improving mechanical performance by reducing organics and increasing WA density [15]. These treatments aim to modify the physical and chemical characteristics of WA, which ultimately govern its behavior in cementitious systems.

The performance of WA in cementitious systems is governed not only by physical characteristics such as particle size and morphology, but also by its chemical reactivity within the cement hydration environment [16]. In particular, its behavior can range from inert filler action to pozzolanic or hydraulic contribution depending on its amorphous phase content, calcium availability, and alkali composition. High levels of alkali oxides (e.g., K_2O, Na_2O) and sulfates can influence early hydration kinetics by accelerating or inhibiting C_3S and C_3A reactions, while soluble salts may affect setting behavior and long-term durability. Conversely, the presence of reactive calcium-bearing or amorphous aluminosilicate phases may enable secondary hydration reactions contributing to strength development [17,18]. Therefore, both physical packing effects and hydration-related contributions should be considered when interpreting compressive strength trends in WA-cement systems.

Despite this body of work, systematic comparative evaluations combining multiple WA types and treatment routes under consistent experimental conditions remain relatively limited. In addition, performance-based indicators such as the Strength Activity Index (SAI) reflect combined physical and potential chemical contributions, which are not separately quantified in this study. This limits the interpretation of the underlying mechanisms behind performance differences and their transferability across different studies and mix designs. Furthermore, while partial replacement of PC with supplementary materials has been reported to reduce global warming potential in concrete depending on substitution rate and material [19], and WA at moderate replacement levels has shown improved compressive and durability properties in some studies [20], comprehensive comparative studies covering multiple WA types and treatment methods under unified testing conditions are still limited.

A previous study by the authors investigated the performance of a single WA type as partial replacement of PC in cement mortars [21]. The materials and experimental dataset of the present study are independent of that work. The present study extends the previous investigation by considering four different WA fractions and systematically evaluating five treatment routes within a consistent experimental framework, using a common 20% replacement level selected based on previous studies reporting favorable performance at similar WA contents. This unified comparison enables the treatment responses of different WA fractions to be evaluated statistically, providing comparative information that was not available from the previous single-ash study. The hypothesis was that the effect of WA treatment on mortar performance would depend on the type and characteristics of the WA fraction.

In this study, the early-age mechanical performance of cement mortars incorporating 20% treated WA as a partial replacement of PC is assessed. Four WA types—fly ash, two bottom ash fractions, and a slag fraction— were subjected to five sequential treatment routes: ball-milling, ball-milling followed by water-washing, ball-milling followed by slaking, ball-milling followed by calcination, and ball-milling followed by water-washing and calcination. Compressive strength was measured at 2, 7, and 28 days, alongside water absorption and ultrasonic pulse velocity (UPV) tests conducted on 7-day cured cement mortars. The SAI was used as a comparative performance indicator. The study provides systematic experimental data on the influence of WA type and treatment route on early-age mechanical behavior in cement mortars, supporting the potential use of WA as a secondary material in cement-based systems.

2. Materials and methods

The present study investigates the influence of using WA as a 20% partial replacement of PC, subjected to five sequential treatment routes comprising ball-milling alone, ball-milling followed by water-washing, ball-milling followed by slaking, ball-milling followed by calcination, and ball-milling followed by water-washing and calcination, on the mechanical and physical properties of hardened mortar specimens. The SAI, based on compressive strength, was used to compare mortar performance. In addition, ultrasonic pulse velocity (UPV) tests and water absorption were determined for 7-day cured specimens to further evaluate early-age material quality and microstructural development.

2.1. WA characterization

The WA were collected from two biomass combustion plants in Latvia. The first WA was obtained from the Liepājas Enerģija Ltd. plant (Latvia), where the average wood combustion temperature was approximately 1000°C. From this plant, both fly ash (L_Fly) and bottom ash were collected. The Liepāja bottom ash was then separated into two fractions: a fine ash fraction and a coarse glassy slag fraction. The bottom ash was sieved using a 2 mm sieve, with the material retained on the sieve collected as the coarse glassy slag fraction (LBC), while the material passing through the sieve was designated as the fine ash fraction (LBF).

The second WA (Oz) was collected from the Ozolnieku KSDU plant (Latvia), with an average combustion temperature of approximately 800°C. The raw Oz fraction was sieved through a 2 mm sieve to remove coarse carbon-rich particles. The as-received WA fractions are shown in Fig. 1.

The chemical composition of WA samples was determined using an X-ray fluorescence (XRF) spectrometer (Rigaku Supermini200) equipped with a 200 W Pd X-ray tube. Measurements were performed under a helium atmosphere.

The crystalline phases of WA samples were characterized by X-ray diffraction (XRD) using an X-ray diffractometer (Aeris, Malvern Panalytical) with CuKα radiation ($\lambda = 1.5406$ Å), operated at 40 kV and 15 mA. Data were collected over a 2θ range of 10–70°, with a step size of 0.02° and a scan rate of 3°/min, corresponding to a nominal scan duration of 20 min. XRD data were analyzed using PANalytical X'Pert HighScore 4.9 software and the International Centre for Diffraction Data (ICDD) PDF-2 database. The diffraction patterns were used for qualitative identification of the crystalline phases present in the investigated WA samples before and after treatment. No quantitative phase analysis or Rietveld refinement was performed.

The morphology, structure, and particle characteristics of the ball-milled WA samples were examined using a scanning electron microscope (SEM) (Thermo Fisher Verios 5 UC). Prior to analysis, the samples were coated with a ~10 nm carbon layer using a LEICA EM ACE 200 coater.

Particle size distribution of the WA samples after the common ball-

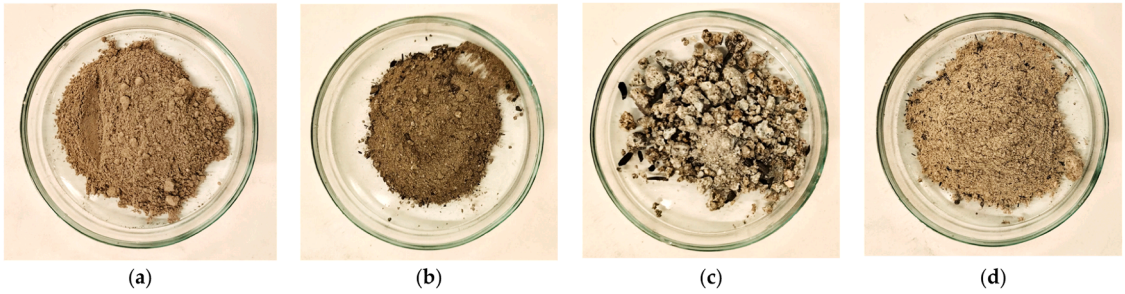

(a) (b) (c) (d)

Fig. 1. Raw WA used in the study: **(a)** L_Fly; **(b)** LBF; **(c)** LBC; **(d)** Oz.

milling step was determined by wet sieving in accordance with Latvian standard LVS EN 933-1:2012 A [22].

Moisture content of the WA samples after the common ball-milling step was determined by oven drying at 105°C for 24 h to constant mass. Loss on ignition (LOI) of the WA samples after the common ball-milling step was measured at 400, 450, and 1000°C. For this purpose, a known mass of WA was placed in pre-weighed crucibles and heated in an air atmosphere at a heating rate of 10°C/min, held at the target temperature for 1 h, and then cooled to room temperature before weighing.

For the ball-milled WA samples, the mass fraction of water-soluble compounds and the pH of the resulting WA–water filtrates were determined. A 5% WA suspension (5 g WA in 95 g deionized water) was prepared and stirred at room temperature for 1 h using a magnetic stirrer. The suspension was then gravity filtered, and the pH of the filtrate was measured using a Hanna HI991003N pH meter. The remaining solid residue was dried at 105°C for 24 h, and its dry mass was determined. The WA dry-mass recovery was calculated as the mass of the recovered WA dry residue relative to the initial dry mass of WA, expressed as a percentage. The mass fraction of water-soluble compounds was then calculated by subtracting the mass of the recovered dry residue from the initial dry mass of WA and expressing the difference as a percentage of the initial dry mass.

2.2. Materials and mixture designs

In this study, PC CEM I 52.5 N from the local manufacturer Schwenk, located in Broceni, Latvia, was used. The PC complied with the European standard LVS EN 197-1:2012 [23]. The chemical composition of the PC is shown in Table 1. Sand from Sakret Ltd., Riga, Latvia, was used as fine aggregate. The sand fraction of 0–2 mm is specifically designed for mortar applications with an optimized particle size distribution [21]. To ensure consistent workability, the flow of all fresh mortar mixtures was maintained within 170–190 mm in accordance with LVS EN 1015-3:2000 [24]. A commercial superplasticizer (Mapei) was used for this purpose, while the water-to-binder ratio was kept constant. The flow-table test was performed using 15 jolts, and three replicate measurements were conducted for each mortar mixture. The reported flow values represent the mean of the three measurements.

Two reference mortar mixtures without WA were prepared to evaluate the effect of the WA treatment methods. In the first reference mixture (REF), only PC was used as the binder. In the second reference mixture (REF_Sand), 20% of the PC was replaced with sand, providing an approximate inert replacement reference at the same replacement level. This mixture served as a reference for comparison with mortars containing treated WA.

Five series of mortars containing treated WA were prepared. The WA was subjected to five different sequential treatment routes:

1) In the first mortar series (L_Fly_5, LBF_5, LBC_5, and Oz_5), the WA fractions were ball-milled for 5 min at 300 rpm by using a Retsch Planetary Ball Mill PM 400 to modify their particle characteristics and morphology [25]. Previous studies have shown that short-duration ball-milling can effectively modify the physical characteristics of WA, including particle size and morphology, while maintaining relatively low processing times [12,26].
2) In the second mortar series (L_Fly_5_W, LBF_5_W, LBC_5_W, and Oz_5_W), the WA fractions were ball-milled for 5 min at 300 rpm and subsequently water-washed to remove water-soluble compounds [8,27]. A total of 100 g of ball-milled WA was mixed with 1 L of tap water, vigorously stirred for 10 min, and then allowed to settle for 12 h. Approximately 800 mL of the leachate was then decanted. Another 1 L of tap water was added to the WA slurry and left for a further 12 h. This procedure was repeated a third time, resulting in a total of three washing cycles. After the final decantation, the WA slurry was dried at 105°C for 24 h. For mortar preparation, the 20% replacement level of PC by water-washed WA was calculated based on the mass of the recovered dried washed ash residue.
3) In the third mortar series (L_Fly_5_S, LBF_5_S, LBC_5_S, and Oz_5_S), the WA fractions were ball-milled for 5 min at 300 rpm and subsequently slaked to mitigate potential expansion associated with free lime [28,29]. After ball-milling, the WA fractions were submerged in water for 24 h using a water-to-ash mass ratio of 1:1. The resulting slurries were then incorporated into the mortar mixtures, with the mixing water adjusted to maintain the target water-to-binder ratio. The amount of water retained within the slaked-ash slurry was not independently quantified, which may have influenced the effective free-water content of the mortar mixtures.
4) In the fourth mortar series (L_Fly_5_t, LBF_5_t, LBC_5_t, and Oz_5_t), the WA fractions were ball-milled for 5 min at 300 rpm and subsequently calcined at 1000°C for 1 h in an air atmosphere with a heating rate of 10°C/min to remove unburned and organic components [14,30]. High-temperature treatment of biomass ashes is commonly used to modify ash composition and mineralogy and to reduce loss on ignition, typically within the temperature range of 800–1000°C. Such treatment promotes the removal of residual carbonaceous material and may lead to the partial decomposition of carbonate phases, depending on ash composition. Therefore, 1000°C was selected as a representative high-intensity treatment condition within the range reported in the literature [17].
5) In the fifth mortar series (L_Fly_5_W_t, LBF_5_W_t, LBC_5_W_t, and Oz_5_W_t), the WA fractions were subjected to a combined water-

Table 1
Chemical composition of PC.

Compound	SiO_2	Al_2O_3	Fe_2O_3	CaO	MgO	SO_3	K_2O	Na_2O	Cl	LOI
Result (w%)	20.0	4.4	3.4	63.0	1.4	2.6	0.4	0.3	0.06	2.3

washing and calcination [15,31]. First, the WA fractions were treated according to the procedure described in the second series. Subsequently, the ball-milled and water-washed WA fractions were calcined following the procedure described in the fourth series.

A schematic overview of the sequential WA treatment routes is presented in Fig. 2.

The mortar compositions and their designations are presented in Table 2, normalized to a 1 kg binder basis. In total, 22 mortar mixtures were prepared. In WA-containing mixtures, 20% of PC by mass was replaced. This replacement level was selected based on previous studies reporting favorable performance at similar WA contents [28].

All WA-containing mixtures were designed with a water-to-binder ratio (W/B) of 0.48, where the binder is defined as the sum of PC and WA. In WA-containing mixtures, partial replacement of PC resulted in a water-to-cement ratio (W/C) of 0.60 due to the reduced cement content in the binder system.

For the REF_Sand mixture, 20% of the PC mass was replaced by sand to provide a non-reactive reference mixture corresponding to the replacement level used for the WA-containing mixtures. Thus, compared with the REF mixture containing 1.00 kg of PC, the REF_Sand mixture contained 0.80 kg of PC and 0.20 kg of additional sand. For consistency with the WA-containing mixtures, the 0.20 kg of sand was considered part of the 1.00 kg cement-replacement basis when calculating the W/B ratio. Accordingly, the REF_Sand mixture had a W/C ratio of 0.60 and a W/B ratio of 0.48.

The REF_Sand mixture was included as an approximate inert replacement reference to evaluate the effect of replacing 20% of PC with a nominally non-reactive material. However, REF_Sand was not intended to fully isolate filler effects, as differences in particle characteristics and superplasticizer demand may also influence mortar behavior.

A sand-to-binder ratio of 2.8 was maintained for all mixtures to provide comparable aggregate proportions. Since WA replacement was performed on a mass basis, differences in specific gravity and particle characteristics between WA, PC, and sand may have influenced the relative solid volume and packing behavior of the mixtures. Accordingly, the investigated mixtures were designed as a screening study of different WA types and treatment routes rather than as a fully volume-matched experimental design.

To achieve comparable fresh-state workability, the superplasticizer dosage was adjusted individually for each mixture. Consequently, the admixture content varied among the investigated mortars. Although this approach allowed similar flow characteristics to be maintained, differences in superplasticizer dosage may also have influenced hydration and strength development. Therefore, the independent influence of superplasticizer dosage cannot be completely separated from the effects of WA type and treatment and should be considered when interpreting the results.

2.3. Ultrasonic pulse velocity and water absorption

Ultrasonic pulse velocity (UPV) measurements were performed using an UltraTest GmbH IP-8 system with 25 kHz transducers in a fixed transmitter–receiver configuration and a 40 mm transducer spacing. For early-age monitoring, fresh cementitious mortars (L_Fly_5 and L_Fly_5_W) were selected because they showed the largest difference in 2-day compressive strength among the corresponding ball-milled and ball-milled/water-washed mixtures. This allowed the influence of water-washing on early-age structural development to be monitored in greater detail using continuous UPV measurements. The mixture compositions correspond to those given in Table 2. Three independently prepared specimens were tested for each mixture. The fresh mortars were cast into cylindrical molds with dimensions of Ø50 mm × 50 mm, lightly compacted to ensure uniform distribution and minimize entrapped air, and sealed with plastic film to prevent moisture loss. Measurements were conducted at room temperature. The transducers were placed in direct contact with the specimen surface without the use of coupling gel. Continuous UPV monitoring started immediately after casting, with measurements recorded at 1-min intervals for 48 h. The results are presented as mean UPV values with standard deviations calculated from the three independent specimens.

In addition, UPV measurements were performed on all hardened mortar specimens at 7 days of curing to assess the developed internal structure at early age. The UPV measurements were conducted on 40 × 40 × 160 mm mortar prisms prepared using the same mixture compositions and proportions as those used for the compressive-strength testing (Table 2). The transducers were placed on two opposite longitudinal side faces of the prisms, with a 40 mm distance between them. Three UPV measurements were then taken at different positions along the 160 mm length of each prism: near one end, at the middle, and near the opposite end. The cast top and bottom faces were not used for UPV measurements. Three independently prepared specimens were tested for each mixture. The measurements were conducted at room temperature, and a thin layer of coupling medium was applied between the transducers and specimen surfaces to ensure adequate acoustic contact. UPV values are reported as mean values with standard deviations calculated from the three independent specimens.

Water absorption was determined on mortar specimens cured for 7 days using the water absorption portion of ASTM C642-21 [32]. Hardened specimens were dried at 105°C for 48 h until constant mass was

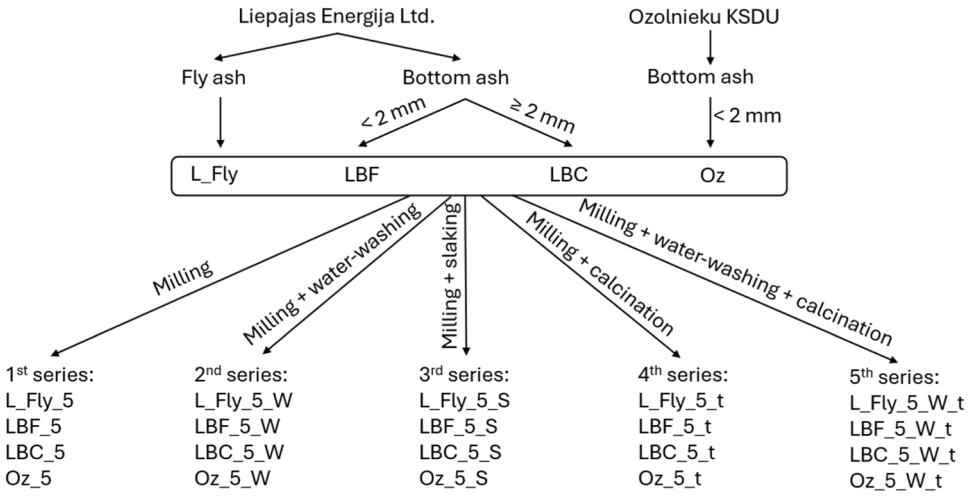

Fig. 2. Schematic overview of the sequential WA treatment routes.

Table 2
The compositions of cement mortars.

Series	Treatment	Sample designations	PC (kg)	WA (kg)	Sand (kg)	Water (kg)	Super-plasticizer (g)	Super-plasticizer (%)	Slump flow (mm)
Reference 1	None	REF	1.00	0.00	2.80	0.48	11	1.1	181
Reference 2	None	REF_Sand	0.80	0.00	3.00	0.48	19	2.4*	178
1	Milling	L_Fly_5	0.80	0.2	2.80	0.48	37	3.7	182
		LBF_5					20	2.0	177
		LBC_5					18	1.8	179
		Oz_5					20	2.0	182
2	Milling + washing	L_Fly_5_W	0.80	0.2	2.80	0.48	33	3.3	183
		LBF_5_W					15	1.5	184
		LBC_5_W					15	1.5	175
		Oz_5_W					15	1.5	173
3	Milling + slaking	L_Fly_5_S	0.80	0.2	2.80	0.48	33	3.3	176
		LBF_5_S					15	1.5	183
		LBC_5_S					15	1.5	180
		Oz_5_S					18	1.8	178
4	Milling + calcination	L_Fly_5_t	0.80	0.2	2.80	0.48	31	3.1	187
		LBF_5_t					15	1.5	181
		LBC_5_t					13	1.3	180
		Oz_5_t					15	1.5	189
5	Milling + washing + calcination	L_Fly_5_W_t	0.80	0.2	2.80	0.48	29	2.9	179
		LBF_5_W_t					15	1.5	180
		LBC_5_W_t					13	1.3	175
		Oz_5_W_t					15	1.5	177

Note: Superplasticizer dosage was calculated relative to the binder/replacement basis. For WA-containing mixtures, this basis was PC + WA (1.00 kg total), whereas for REF_Sand, the dosage was calculated relative to the PC mass (0.80 kg), as quartz sand is a non-cementitious material.

reached, then cooled to room temperature in a desiccator and weighed. The specimens were subsequently immersed in water at room temperature for 72 h until constant mass was achieved. Water absorption was calculated as the percentage mass increase after immersion relative to the dry mass. The same three specimens used for the 7-day UPV measurements were subsequently used for the water absorption test.

2.4. Compressive strength of hardened mortar samples

Compressive strength for all mortar samples was determined according to the LVS EN 196-1:2016 [33]. Mortar samples were produced in 40 × 40 × 160 mm molds made of steel. The hardened mortar samples were demolded 24 h after production and placed in water. The compressive strength measurements were performed after 2, 7, and 28 days. The compressive test was performed on 62.5 × 40 × 40 mm mortar samples with the speed of 0.8 MPa/s using a Controls 3000 kN compression machine [21]. Six specimens were tested for each mixture and curing age, and the results were reported as mean values with standard deviations.

2.5. Statistical analysis

Statistical analysis was performed to determine whether the observed differences in compressive strength among the investigated mortar mixtures were statistically significant. Analyses were conducted separately for each curing age (2, 7, and 28 days), using the six replicate measurements obtained for each mixture. For each curing age, a one-way analysis of variance (ANOVA) was performed with mortar mixture as the factor. When the ANOVA indicated statistically significant differences among the mixture means, Tukey's honestly significant difference (HSD) post-hoc test was applied for pairwise comparisons. Statistical significance was evaluated at a significance level of $\alpha = 0.05$. The results of the Tukey HSD analysis are presented as compact letter groupings, where mixtures sharing at least one letter are not significantly different, whereas mixtures that do not share any letter differ significantly at the 5% significance level. All statistical analyses were performed using R version 4.6.1 in RStudio.

3. Results and discussion

3.1. XRF and XRD of ball-milled WA

XRF results are shown in Table 3, while the XRD patterns of the investigated ball-milled WA samples are presented in Fig. 3. The L_Fly_5 sample exhibits reflections attributable to arcanite (K_2SO_4; PDF 00-044-1414), calcite ($CaCO_3$; PDF 00-005-0586), and quartz (SiO_2; PDF 01-089-1961). The Oz_5 ash exhibits reflections attributable to quartz, lime (CaO; PDF 01-082-1690), and calcite. The LBF_5 and LBC_5 samples show similar XRD patterns, with reflections attributable to quartz together with pseudowollastonite ($CaSiO_3$; PDF 01-074-0874).

The identified crystalline phases demonstrate differences in the initial mineralogical composition of the investigated WA. These initial mineralogical characteristics provide a reference for evaluating the changes induced by water-washing, slaking, and calcination.

3.2. SEM images of ball-milled WA

The SEM images of WA after the first treatment procedure (5 min at 300 rpm ball-milling) are shown in Fig. 4. The L_Fly_5 sample (Fig. 4a) exhibits a more fragmented particle appearance compared with the other investigated ashes, although agglomeration of particles is also observed. The LBF_5, LBC_5, and Oz_5 samples (Fig. 4b–d) consist of irregularly shaped particles with smaller fragments attached to larger particles [34]. Surface pores are observed in LBF_5 and Oz_5 (Fig. 4b,d), whereas LBC_5 (Fig. 4c) exhibits a comparatively smoother particle surface [35]. The SEM images reveal differences in the particle morphology of the investigated ashes depending on the WA type.

3.3. Moisture content and LOI values of ball-milled WA

WA can absorb ambient moisture due to its relatively high surface area and porosity [7]. The amount of physically adsorbed water was determined as the difference between the initial mass of the WA sample and the mass after drying at a temperature slightly above the water evaporation point. The same principle is applied in the determination of loss on ignition (LOI). At higher temperatures, mass loss is associated with processes such as the decomposition of organic matter, the release of chemically bound water, and the decomposition of calcium and

Table 3
Chemical composition of L_Fly_5, LBF_5, LBC_5 and Oz_5.

Compound	SiO_2	CaO	Al_2O_3	SO_3	Fe_2O_3	K_2O	MgO	P_2O_5	MnO	Na_2O	Cl	ZnO
L_Fly_5	4.2	26.2	1.5	21.4	1.3	23.8	6.4	6.1	0.8	2.2	3.2	2.5
LBF_5	49.6	24.2	5.6	2.8	1.8	6.8	3.4	3.6	0.3	1.2	0.3	0.1
LBC_5	60.1	19.6	5.9	0.3	1.6	5.2	3.5	1.9	0.3	1.4	0	0
Oz_5	15.4	56.6	1.8	2.1	1.4	7.4	9.7	4.9	0.2	0	0.1	0.1

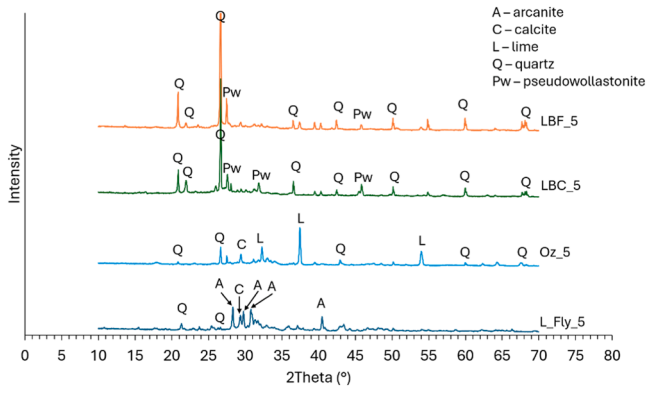

Fig. 3. XRD patterns of L_Fly_5, Oz_5, LBC_5 and LBF_5.

magnesium carbonates [36]. The moisture content and LOI values of L_Fly_5, LBF_5, LBC_5, and Oz_5 are given in Table 4.

The highest mass loss was observed for L_Fly_5, which may be associated with the relatively high porosity and specific surface area commonly reported for wood fly ash [37] as well as a potentially higher content of organic matter and volatile fractions commonly present in fly ash [38]. The lowest moisture content and LOI values were observed for LBC_5.

3.4. Mass percentage of water-soluble compounds and pH of the filtrate

The mineralogical and chemical composition of wood biomass ashes can vary depending on several factors, such as wood species, combustion method, and temperature [8]. The presence of water-soluble compounds in WA influences the pH of WA–water filtrates. The mass percentage of ball-milled WA dry-mass recovery, water-soluble compounds, and the pH of filtrates obtained after 1 h of stirring are presented in Table 5.

Fig. 5 shows water-soluble salts obtained by drying the leachate of L_Fly_5 after the water-washing procedure.

The obtained salts consisted of white flakes (Fig. 5a). The SEM image (Fig. 5b) revealed the presence of hexagonal plate-like crystals. These water-soluble salts accounted for 44.4% of the total mass of L_Fly_5, while the corresponding L_Fly_5 dry-mass recovery after washing was 55.6%.

Table 4
Moisture content and LOI values of ball-milled WA.

Sample	Moisture (105°C, 24 h), %	LOI (10°C/min, air), %		
		400°C	450°C	1000°C
L_Fly_5	0.5	1.0	1.3	8.9
LBF_5	0.1	0.3	0.3	3.4
LBC_5	0.02	0.1	0.1	1.1
Oz_5	0.6	0.5	0.5	5.8

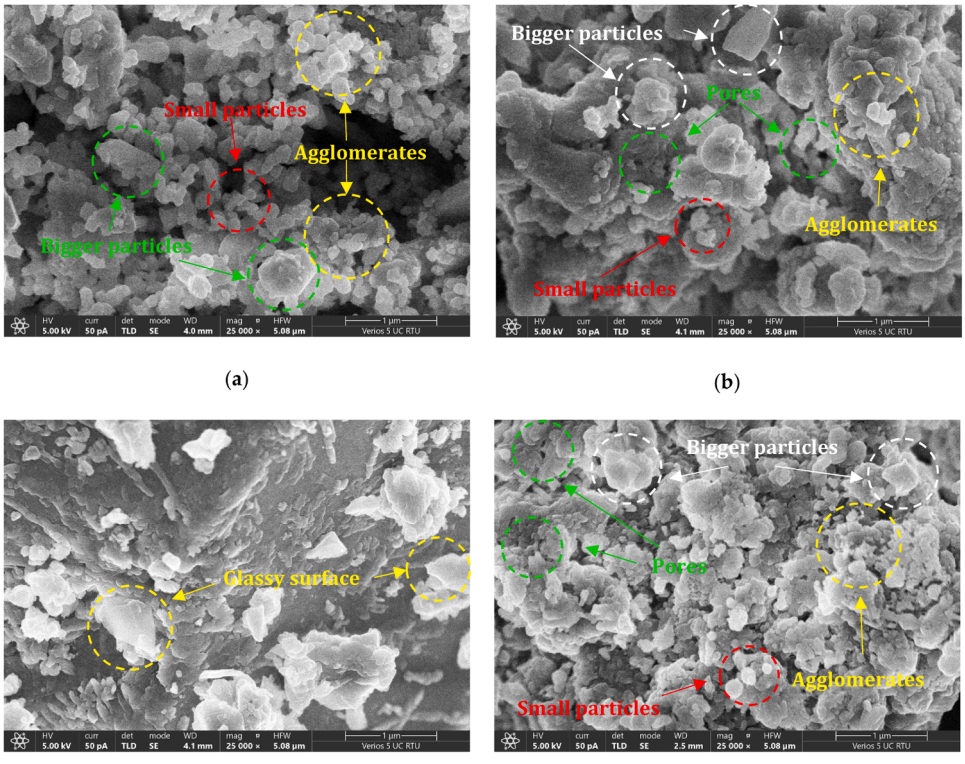

Fig. 4. SEM images of: (**a**) L_Fly_5; (**b**) LBF_5; (**c**) LBC_5; (**d**) Oz_5.

Table 5
Water-soluble compound mass% and the pH of the filtrate.

WA	WA dry-mass recovery, %	Water-soluble compounds, %	pH of filtrate
L_Fly_5	55.6	44.4	12.9
LBF_5	95.0	5.0	12.0
LBC_5	97.4	2.6	11.6
Oz_5	93.2	6.8	12.3

The highest water solubility was observed for L_Fly_5, whose soluble compounds likely contributed to the highest pH value of the filtrate among all WA. Ottosen et al. [8] reported a total solubility of 28.0% for fly ash. Wood biomass fly ash often contains higher amounts of sodium and potassium compounds, which are frequently water-soluble and contribute to increased alkalinity in WA–water systems [39]. The higher soluble mass fraction of L_Fly_5 may also be associated with a greater content of organic compounds [37], which are typically more abundant in fly ash than in bottom ash and exhibit high water solubility [38]. In contrast, LBC_5 showed the lowest water solubility and filtrate pH. Vu et al. [40] reported an average water solubility of 6.9% for wood ash, which is comparable to the values of 5.0% and 6.8% obtained for LBF_5 and Oz_5, respectively, in this study. The pH values of LBF_5 and Oz_5 were 12.0 and 12.3, respectively, with the slightly higher pH of Oz_5 attributed to its higher CaO content. Similar trends in solubility and pH have been reported in previous studies, where fly ash exhibits higher values than bottom ash [8,37,38]. Comparable pH values of 12.1 and 12.3 were also reported by Rahman et al. [41] for 4% and 6% WA–water suspensions, respectively.

3.5. Particle size distribution of ball-milled WA

The particle size distribution of L_Fly_5, LBF_5, LBC_5, and Oz_5 was determined using a wet sieving procedure based on differential sieve weighing. A 100 g sample of WA was passed through a series of sieves with different mesh sizes under a water flow. After sieving, the material retained on each sieve was dried at 105°C for 1.5 h and weighed. The particle size distribution results are shown in Fig. 6.

L_Fly_5 exhibited the finest particle size, with all particles passing through the 0.063 mm sieve. The particle size distributions of the bottom ash samples LBF_5, LBC_5, and Oz_5 were similar. The most pronounced milling effect was observed for LBC_5, which had the coarsest initial particle size (Fig. 1). Similar particle size distributions have been reported in other studies using sieving methods [42,43].

3.6. Effects of treatment methods on WA mineralogical composition

Fig. 7 shows the changes in WA XRD patterns for each WA type subjected to the investigated sequential treatment routes, including initial ball-milling followed by water-washing, slaking, calcination, or combined water-washing and calcination. The XRD measurement duration was 20 min.

The L_Fly_5 sample (Fig. 7a) exhibits reflections attributable to arcanite (PDF 00-044-1414), together with calcite (PDF 00-005-0586) and minor quartz (PDF 01-089-1961). Following water-washing of the ball-milled ash (L_Fly_5_W), reflections attributable to arcanite become less apparent, which is consistent with the dissolution of water-soluble sulfate-bearing phases. Following slaking of the ball-milled ash (L_Fly_5_S), the XRD pattern is generally comparable to that of the corresponding ball-milled sample L_Fly_5. Following calcination of the ball-milled ash (L_Fly_5_t), calcite reflections are no longer observed, while reflections attributable to wollastonite ($CaSiO_3$; PDF 01-076-0186) are detected. Following water-washing and subsequent calcination of the ball-milled ash (L_Fly_5_W_t), reflections attributable to lime (PDF 01-082-1690) and wollastonite are observed.

The LBF_5 and LBC_5 samples (Fig. 7b,c) exhibit similar XRD patterns, with reflections attributable to quartz together with minor pseudowollastonite ($CaSiO_3$; PDF 01-074-0874). Following water-washing or slaking of the ball-milled ashes, no substantial qualitative changes are observed in the detectable crystalline phases. Following calcination, with or without prior water-washing, reflections attributable to gehlenite ($Ca_2Al_2SiO_7$; PDF 01-079-1726) are observed, while quartz reflections remain present.

The Oz_5 sample (Fig. 7d) exhibits reflections attributable to quartz and lime, together with calcite. Following water-washing of the ball-milled ash (Oz_5_W), lime reflections are no longer observed, which is consistent with hydration of CaO during contact with water. Following slaking of the ball-milled ash (Oz_5_S), reflections attributable to portlandite ($Ca(OH)_2$; PDF 01-078-0315) are observed, while lime

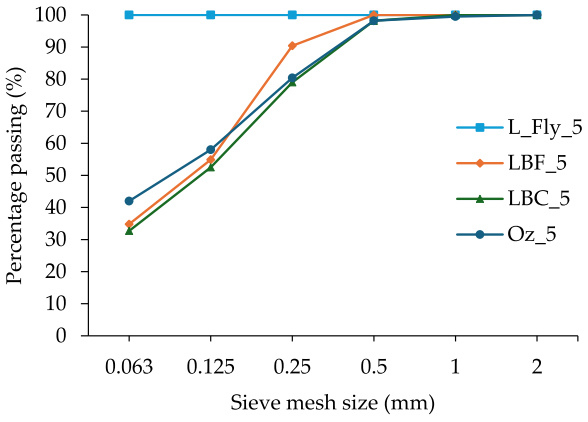

Fig. 6. Particle size distribution of L_Fly_5, LBF_5, LBC_5, and Oz_5.

(a) (b)

Fig. 5. Images of water-soluble salts separated from L_Fly_5: (a) camera image; (b) SEM image.

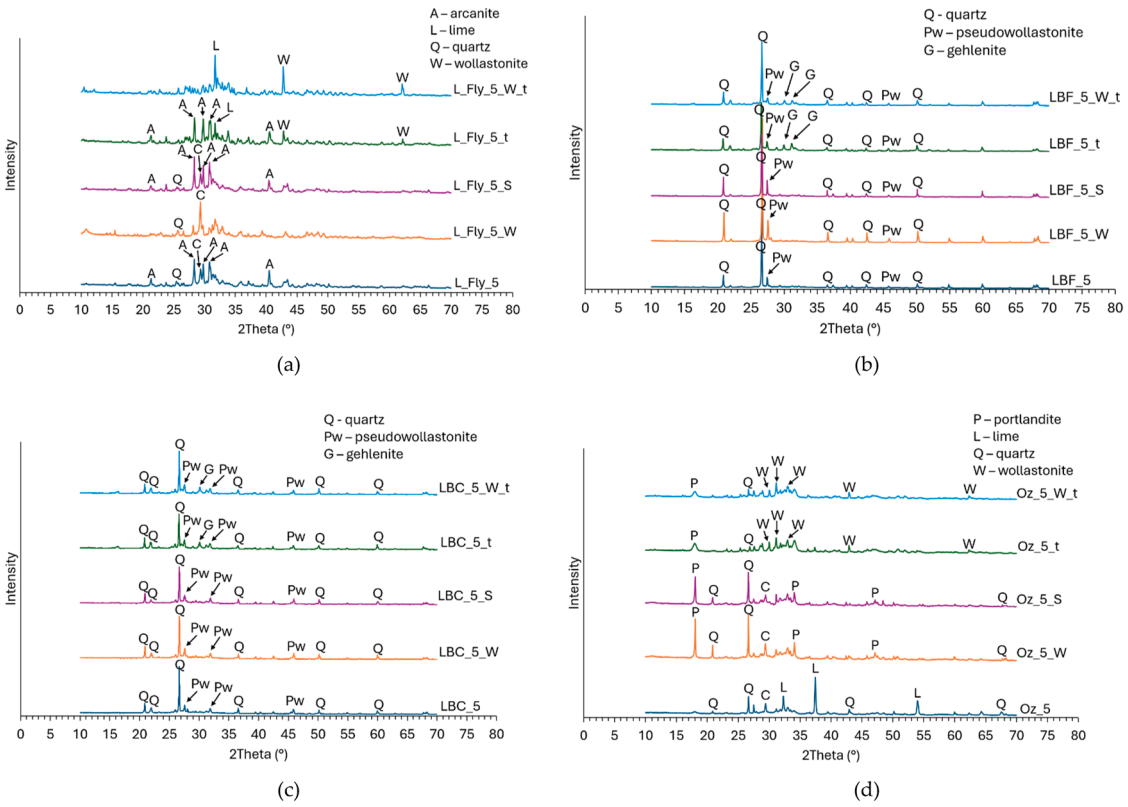

Fig. 7. XRD patterns of ball-milled WA samples and samples subjected to subsequent treatments: (a) L_Fly, (b) LBF, (c) LBC, and (d) Oz.

reflections are no longer detected. Following calcination, with or without prior water-washing, reflections attributable to wollastonite are observed. Minor portlandite reflections are also detected after calcination, which may be associated with hydration of residual CaO during cooling.

3.7. Influence of water-washing on early-age UPV development and stiffening behavior of wood fly ash mortars

UPV is a non-destructive technique used to monitor changes in the internal structure of cementitious materials. As hydration progresses, the formation and interconnection of hydration products generally increase the stiffness and continuity of the solid skeleton, resulting in higher ultrasonic wave velocities. Therefore, UPV provides indirect information on setting, stiffening, and early-age microstructural development.

The UPV curves of REF, REF_Sand, L_Fly_5, and L_Fly_5_W are shown in Fig. 8, illustrating the evolution of internal structural development in the mortars during the early curing period. The REF mixture exhibits the most rapid increase in UPV, with a steep initial rise within the first hours and a plateau of approximately 4100–4200 m/s after ~36–48 h, consistent with the development of a relatively continuous and stiff internal structure. REF_Sand follows a similar trend but with slightly lower UPV values throughout the testing period, stabilizing at a lower final plateau of approximately 3900–4000 m/s. This difference may be associated with the different mixture composition and lower PC content in the REF_Sand system.

In contrast, L_Fly_5 shows significantly delayed and reduced UPV development, with a gradual and nearly linear increase over time and no clear inflection point, reaching approximately 2200 m/s at 48 h. The lower UPV values are consistent with a less developed and less continuous internal structure at early age. A similar influence of wood fly ash on UPV development has been reported in previous studies [44,45]. However, these studies evaluated UPV at selected curing ages, whereas

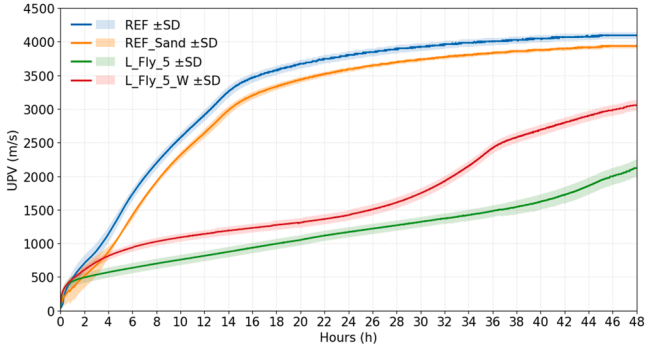

Fig. 8. Evolution of UPV in REF, REF_Sand, L_Fly_5, and L_Fly_5_W mortars.

the present study continuously monitored UPV during the early-age period, providing a more detailed description of its development over time. This behavior may be related to the high content of water-soluble alkali and sulfate compounds present in the wood fly ash, which may affect the early development of the cementitious matrix.

L_Fly_5_W exhibits a clear difference compared with L_Fly_5, showing higher UPV values and a more pronounced increase during the later stages of testing (around 30–36 h), reaching approximately 3000 m/s at 48 h. This difference indicates a faster increase in UPV during the early-age period after water-washing. The observed improvement may be associated with the removal of water-soluble compounds during washing, although UPV measurements alone do not allow the specific contribution of individual compounds or hydration processes to be established. The slightly lower superplasticizer dosage used for L_Fly_5_W (3.3% compared with 3.7% for L_Fly_5) may also have contributed to the difference in early-age UPV development and should therefore be considered when interpreting the effect of water-washing.

3.8. Water absorption and UPV of 7-day cured mortars

The water absorption and UPV of 7-day cured mortars are shown in Fig. 9 and are used to assess differences in internal structure and water transport properties. In general, higher UPV values are associated with a more continuous and stiffer internal structure, while higher water absorption reflects greater accessible porosity. The reference systems REF and REF_Sand exhibit the highest UPV values and the lowest water absorption, suggesting comparatively lower internal porosity and greater structural continuity. In contrast, the ball-milled fly ash mortar (L_Fly_5) shows the lowest UPV and the highest water absorption, which may indicate a relatively more porous and less developed internal structure (Fig. 9a). Water-washing of the fly ash (L_Fly_5_W) resulted in an increase in UPV and a reduction in water absorption, suggesting improved matrix continuity and lower accessible porosity. This observation is also consistent with the early-age UPV results (Fig. 8), which showed higher UPV values for L_Fly_5_W. The XRD results provide additional context for this difference, as the arcanite reflections observed in L_Fly_5 became less apparent after water-washing (Fig. 7a), suggesting the removal of water-soluble sulfate-bearing phases. Thus, the compositional change identified by XRD is consistent with the higher UPV and lower water absorption observed for L_Fly_5_W, although the XRD and UPV results alone do not establish a direct causal relationship between the removal of these phases and the measured properties.

The LBF, LBC, and Oz systems (Fig. 9b–d) show relatively small differences in both UPV and water absorption among the applied treatments, showing less pronounced differences in the measured properties compared to the fly ash system. Although minor variations are observed, no clear systematic relationship between treatment type, UPV, and water absorption can be identified. This relatively limited response is also consistent with the XRD results, which showed no substantial qualitative changes in the detectable crystalline phases of LBF_5 and LBC_5 following water-washing or slaking (Fig. 7b,c). For the Oz system, water-washing resulted in the disappearance of the lime reflections in the XRD pattern (Fig. 7d), which may reflect hydration of CaO during contact with water; however, this change was not accompanied by a pronounced difference in UPV or water absorption among the treatments. Nevertheless, the bottom ash mortars generally exhibit lower water absorption and higher UPV values than L_Fly_5, suggesting a more continuous and less porous internal structure.

The results indicate that water-washing produced the most pronounced changes in UPV and water absorption for the fly ash system, whereas its effect on the bottom ash mortars was comparatively limited.

3.9. Mechanical strength of hardened mortar samples

The compressive strength of the hardened mortar specimens was determined at 2, 7, and 28 days. To evaluate the influence of treated WA on mortar performance, the SAI was calculated based on compressive strength results. The SAI provides a comparative measure of the contribution of WA to the mechanical performance of the mortars. The SAI values were calculated using Eq. (1) [14].

$$SAI\ (\%) = \frac{f_{c-WA}}{f_{c-REF}} \cdot 100\% \quad (1)$$

where:

- f_{c-WA} is the average compressive strength of mortar specimens containing WA;
- f_{c-REF} is the average compressive strength of reference mortar specimens without WA.

The compressive strength values of the hardened mortar specimens at 2, 7, and 28 days, together with the corresponding standard deviations, percentage increase between curing ages, and Tukey HSD grouping letters, are presented in Table 6. The reported compressive strength values represent the average of six individual measurements for each mixture and curing age, while the standard deviations were calculated from these six measurements and represent the experimental variability within each mixture.

To assess whether mixture composition significantly affected

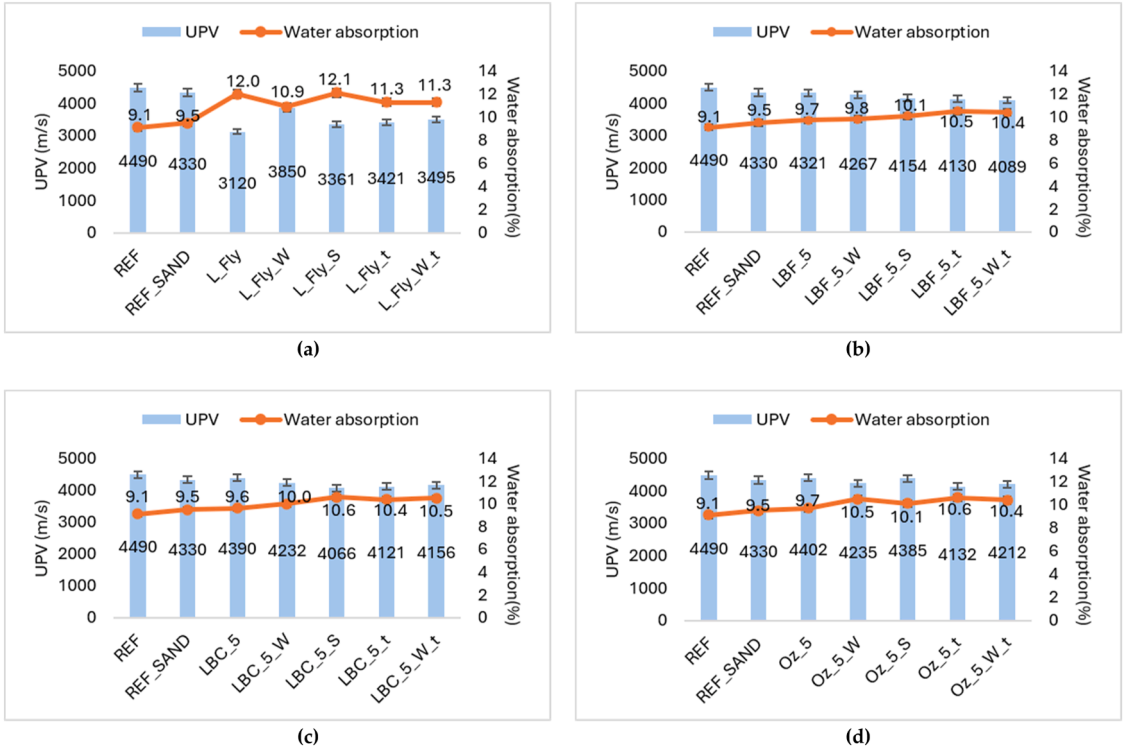

Fig. 9. UPV and water absorption of 7-day cured mortars.

compressive strength, one-way analysis of variance (ANOVA) was performed separately for each curing age (2, 7, and 28 days). The ANOVA results are summarized in Table 7. The degrees of freedom (DF) are reported for the mixture effect and error term, respectively. A statistically significant effect of mixture composition was observed at all investigated curing ages ($p < 0.001$). Therefore, pairwise comparisons were subsequently performed using Tukey's honestly significant difference (HSD) test at a significance level of $\alpha = 0.05$. Mixtures sharing the same letter are not statistically significantly different, whereas mixtures assigned to different letter groups exhibit statistically significant differences in compressive strength.

The compressive strength of REF at 2, 7 and 28 days was 33, 45 and 56 MPa, respectively. Across all mixtures, none of the specimens reached compressive strength values comparable to those of REF.

The SAI values were calculated using the mean compressive strength of the REF mortar at each curing age as the reference value. For each WA-containing mixture, the SAI was calculated individually from the six measured compressive strength values, while the corresponding mean strength of the REF mortar was used as the denominator. The error bars shown in Figure 10 represent the standard deviation of the six calculated SAI values.

Figure 10 presents the strength activity index (SAI) of the hardened mortar mixtures at curing ages of 2, 7, and 28 days.

After 28 days, REF_Sand reached 63% of the compressive strength of REF. Among the WA-containing mixtures, LBF_5 and Oz_5 exhibited the highest compressive strength values (38.1 and 39.4 MPa, respectively), both belonging to Tukey HSD group b, whereas REF_Sand and LBC_5 were assigned to group c (Table 6). These results indicate statistically higher compressive strength for LBF_5 and Oz_5 compared with REF_Sand, while LBC_5 showed comparable performance. Correspondingly, these mixtures exhibited SAI values of 69%, 65%, and 71% for LBF_5, LBC_5, and Oz_5, respectively (Fig. 10b–d). The results suggest that these specific ball-milled bottom ash mixtures exhibited comparatively higher performance under the investigated conditions. The higher strength may be related to differences in their intrinsic characteristics; however, the individual contribution of factors such as particle packing, chemical composition, and reactivity was not directly quantified in the present study.

Table 6
Compressive strength of mortar mixtures and Tukey HSD grouping.

Sample	Compressive strength (MPa)		
	2 days	7 days	28 days
REF	33.0 ± 0.6^{a}	45.1 ± 0.5^{a}	55.6 ± 0.7^{a}
REF_Sand	18.1 ± 0.8^{efghi}	31.1 ± 0.7^{b}	35.0 ± 0.9^{c}
L_Fly_5	4.1 ± 0.5^{l}	17.2 ± 0.8^{l}	22.4 ± 0.7^{j}
L_Fly_5_W	20.3 ± 1.1^{cd}	27.2 ± 1.0^{ef}	33.3 ± 0.5^{d}
L_Fly_5_S	13.3 ± 0.8^{k}	19.1 ± 1.2^{k}	23.6 ± 0.7^{ij}
L_Fly_5_t	17.4 ± 0.5^{ghij}	19.1 ± 0.7^{k}	24.1 ± 0.5^{i}
L_Fly_5_W_t	16.2 ± 0.9^{j}	17.0 ± 0.6^{l}	20.2 ± 0.6^{k}
LBF_5	19.8 ± 0.5^{cde}	30.5 ± 0.6^{bc}	38.1 ± 0.8^{b}
LBF_5_W	19.7 ± 1.1^{cde}	28.3 ± 0.6^{de}	35.3 ± 0.6^{c}
LBF_5_S	19.8 ± 0.5^{cde}	26.2 ± 0.4^{fg}	31.1 ± 0.9^{efg}
LBF_5_t	18.7 ± 0.8^{defgh}	25.2 ± 0.8^{gh}	31.1 ± 0.6^{efg}
LBF_5_W_t	18.4 ± 0.5^{efgh}	24.9 ± 0.7^{gh}	31.3 ± 0.4^{efg}
LBC_5	19.8 ± 1.1^{cde}	30.3 ± 0.3^{bc}	35.9 ± 0.3^{c}
LBC_5_W	19.6 ± 1.7^{cde}	27.4 ± 0.4^{ef}	32.3 ± 0.7^{de}
LBC_5_S	18.1 ± 0.8^{efghi}	24.1 ± 0.9^{hi}	30.9 ± 0.8^{efg}
LBC_5_t	16.6 ± 0.9^{ij}	22.1 ± 0.4^{j}	31.5 ± 0.5^{ef}
LBC_5_W_t	16.9 ± 0.7^{hij}	23.2 ± 0.5^{ij}	30.1 ± 0.7^{fg}
Oz_5	21.0 ± 0.7^{c}	31.2 ± 0.6^{b}	39.4 ± 0.6^{b}
Oz_5_W	19.1 ± 0.8^{defg}	27.9 ± 0.6^{e}	30.0 ± 0.9^{g}
Oz_5_S	22.8 ± 0.5^{b}	29.3 ± 0.7^{cd}	35.5 ± 0.9^{c}
Oz_5_t	19.3 ± 1.1^{cdef}	24.1 ± 0.7^{hi}	28.3 ± 0.6^{h}
Oz_5_W_t	17.5 ± 0.5^{fghij}	22.1 ± 0.3^{j}	30.3 ± 0.8^{fg}

Note: Values are presented as mean ± standard deviation (n = 6). Different superscript letters within the same curing-age column indicate statistically significant differences according to Tukey's HSD test ($\alpha = 0.05$). Statistical comparisons were performed separately for each curing age.

Table 7
One-way ANOVA results for differences in compressive strength among mortar mixtures at different curing ages.

Curing age	DF (Mixture, Error)	F-value	p-value
2 days	21, 110	196.0	<0.001
7 days	21, 110	517.0	<0.001
28 days	21, 110	686.0	<0.001

In contrast, most fly ash-containing mixtures exhibited lower compressive strength than the highest-performing bottom ash-based mixtures (Fig. 10a). The fly ash mixtures were generally assigned to lower Tukey HSD groups, indicating statistically lower strength than LBF_5 and Oz_5. Among the fly ash mixtures, L_Fly_5 exhibited the lowest early-age compressive strength (4.1 MPa at 2 days). Reduced early-age performance of wood fly ash has also been reported in previous studies and may depend on ash origin, composition, and processing conditions. In contrast, Fořt et al. [46] reported a substantially higher SAI value (87% at 28 days) for wood fly ash at 20% cement replacement, which the authors associated with a higher content of reactive SiO_2 and Al_2O_3. The lower performance of L_Fly_5 may therefore be related to differences in the intrinsic characteristics of the investigated ash.

The ball-milling followed by water-washing treatment resulted in a substantial increase in the compressive strength of L_Fly_5 at all investigated curing ages. Compared with L_Fly_5, the compressive strength of L_Fly_5_W increased from 4.1 to 20.3 MPa at 2 days, from 17.2 to 27.2 MPa at 7 days, and from 22.4 to 33.3 MPa at 28 days. The two mixtures were assigned to different Tukey HSD groups at all curing ages, confirming that the differences in compressive strength were statistically significant. The improvement associated with washing may be related to changes in the soluble fraction; however, this mechanism requires further verification. The XRD results provide additional context for this observation, as the reflections attributable to arcanite became less apparent after water-washing of L_Fly_5 (Fig. 7a), suggesting the removal of water-soluble sulfate-bearing phases. However, this XRD observation alone does not establish that the removal of these phases was responsible for the observed increase in compressive strength.

The ball-milling followed by calcination treatment did not result in a consistent increase in compressive strength compared with the other investigated treatment routes. This suggests that the applied thermal treatment conditions did not provide a measurable improvement in WA contribution to strength development. Similar observations regarding the limited benefits of thermal treatment of biomass ashes have been reported previously [14,47].

The effect of ball-milling followed by slaking was generally limited and did not result in a consistent improvement compared with ball-milling followed by water-washing. The influence of slaking depended on the ash type and curing age, with some slaked mixtures showing comparable performance to their water-washed counterparts, while others exhibited statistically different strength values according to Tukey HSD analysis. The higher 28-day compressive strength observed for Oz_5_S compared with Oz_5_W may be related to the intrinsic characteristics of this ash, including its relatively high CaO content, which can participate in hydration and carbonation processes in CaO-rich biomass ash systems [48]. However, this mechanism was not directly evaluated in the present study.

The combination of ball-milling followed by water-washing and calcination did not consistently improve compressive strength compared with the corresponding treatment routes involving ball-milling alone or ball-milling followed by water-washing, slaking, or calcination. At 28 days, the combined ball-milling followed by water-washing and calcination treatment resulted in statistically lower compressive strength than the corresponding ball-milled mixtures for all four ash types according to Tukey's HSD test. Compared with the corresponding mixtures subjected to ball-milling followed by water-washing, the combined

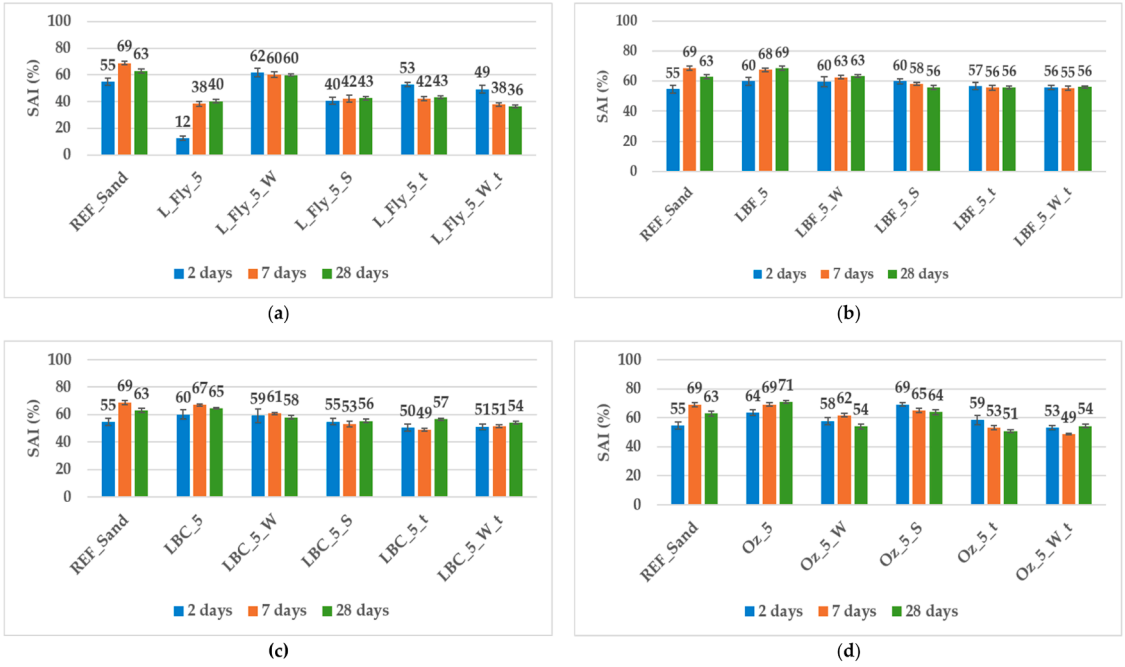

Fig. 10. SAI of hardened mortar specimens containing treated WA: (a) L_Fly; (b) LBF; (c) LBC; (d) Oz.

treatment resulted in statistically lower strength for L_Fly and LBF, whereas the differences were not statistically significant for LBC or Oz. Thus, the combined ball-milling followed by water-washing and calcination route did not provide a consistent strength advantage over the other treatment routes under the investigated conditions.

Although differences in compressive strength were observed among the investigated treatment routes, the contribution of other mixture-related factors should also be considered when interpreting these results. In particular, the superplasticizer dosage was adjusted individually to achieve comparable fresh-state workability and therefore varied between mixtures. Furthermore, WA replacement was performed on a mass basis, while the investigated WA materials differ from PC in terms of specific gravity and particle characteristics, which may have influenced the effective solid volume and particle packing behavior within the mixtures. Consequently, the observed differences in compressive strength should be interpreted as the combined effect of WA characteristics, treatment route, and mixture design parameters rather than being attributed exclusively to the applied treatment.

The 75% strength activity index requirement specified in ASTM C618 for fly ash and natural pozzolans was used only as a comparative benchmark to contextualize the performance of the investigated WA mixtures, since ASTM C618 was developed for conventional supplementary cementitious materials and no dedicated internationally recognized standard currently exists for the use of biomass ashes as supplementary cementitious materials. The compressive strength measurements in the present study were performed according to LVS EN 196-1:2016; therefore, the investigated WA mixtures were not evaluated for compliance with ASTM C618 requirements, and the comparison with the 75% threshold should be interpreted only as an indicative reference value rather than a demonstration of ASTM C618 compliance. After 28 days of curing, none of the investigated WA-containing mixtures reached this comparative benchmark.

A comparison with previous studies further highlights the relatively limited contribution of the investigated WA to compressive strength development. In the present study, SAI values ranged approximately between 12% and 71% at 20% PC replacement, with all mixtures remaining below the 75% threshold specified in ASTM C618. In contrast, higher performance has been reported in the literature depending on WA type and treatment conditions (Table 8). For example, Tiegoum Wembe et al. [42,43] reported SAI values of up to 91% at 28 days for ground WA, while Teker Ercan et al. [12] achieved SAI values of up to 96% following short-duration ball-milling. Similarly, Rosales et al. [15] reported SAI values exceeding 100% for treated olive biomass bottom ash.

The comparison with previous studies indicates that the performance of WA as a partial replacement of PC is highly dependent on both the intrinsic characteristics of WA and the applied treatment method. In the present study, none of the investigated sequential treatment routes resulted in a consistent improvement in early-age compressive strength. The results suggest that the observed behavior is governed by the combined effects of cement dilution and the limited contribution of the investigated WA to early-age strength development. At the applied replacement level of 20%, the reduction in cement content likely plays a dominant role in early-age performance, while the applied treatments were not sufficient to offset this effect. Consequently, the studied ashes appear to provide a limited contribution to strength development within the first 28 days of curing.

Since compressive strength was evaluated only up to 28 days, any potential contribution to later-age strength development remains unverified. Therefore, the present findings should be regarded as a screening-level assessment of early-age performance rather than a definitive evaluation of long-term suitability as partial PC replacements. The study did not include calorimetry, FTIR, or TGA analyses; thus, mechanistic interpretations are based on compressive strength, water absorption, UPV results, and literature evidence.

3.10. *Engineering context and limitations of the study*

The present study provides a comparative laboratory-scale assessment of WA as a partial replacement for PC in mortar systems. The investigated WA fractions and sequential treatment routes were evaluated based on compressive strength development up to 28 days, SAI, UPV, and water absorption. The results demonstrate that the investigated WA fractions showed different performance depending on their origin and processing history, with differences in chemical composition and mineralogy potentially contributing to their behavior in cement-based systems. From an engineering perspective, WA may be relevant for further investigation in non-structural cement-based products, low-

Table 8
Comparison of treatment methods and SAI values reported for WA as partial replacement of PC.

Study	Type of WA	Replacement	Treatment	Key strength / SAI results	Main observations
This study	Wood ashes (fly + bottom ash)	20%	5 min ball-milling; subsequent washing, slaking, calcination (1000°C, 1 h)	SAI: 12–71% (varies by ash), all < 75%	Low relative strength performance under the investigated conditions; bottom ash generally performs better than fly ash; treatment effects depend on WA type and treatment route
Tiegoum Wembe et al. [42,43]	Wood ash (multiple types of bottom ash)	20%	Sieved / ground	SAI up to 78% (7 d), 91% (28 d) best case	Better performance than present study; ash variability important
Teker Ercan et al. [12]	Wood ash (2 types)	20%	Ball milling 10–20 min	SAI ~90–96% (28 d)	Short milling significantly improves performance; optimal ~10 min
Berra et al. [11]	Woody biomass fly ash	15%	Washing only	SAI ~84% (28 d), ~94% (96 d)	Washing improves long-term strength; delayed benefits
Couto et al. [14]	Eucalyptus wood ash	20%	Grinding (30 min–3 h), calcination 600–800°C	SAI 63–83%; best at long grinding, calcination reduces strength at high T	Mechanical activation more effective than high-T treatment
Kim et al. [49]	Wood biomass fly ash	20%	800°C calcination + 20 min milling	SAI increased from ~70% to ~81%	Combined treatment improves density and strength
Rosales et al. [15]	Olive biomass bottom ash	10%	Washing + 600°C calcination	SAI 82–104%	Strong improvement due to impurity removal and densification

strength concretes, mortars, and other binder systems where moderate mechanical performance and reduced PC consumption are desired. Previous studies have investigated WA as a partial PC replacement in mortar [6,18], as well as its use in application-oriented products such as paver blocks and roof tiles [50]. The potential valorization of WA in cement-based materials is also consistent with broader bioeconomy and circular-economy approaches, where biomass-derived residues are redirected towards value-added applications [51].

The results obtained in this study should be interpreted as a screening-level evaluation of WA performance under controlled laboratory conditions rather than as a demonstration of practical engineering applicability. Although some bottom-ash-based mixtures showed comparatively higher mechanical performance, the investigated materials were assessed only at a single replacement level of 20% PC and up to 28 days of curing. Furthermore, the 75% SAI value specified in ASTM C618 was used as a comparative benchmark, and none of the investigated WA mixtures reached this reference value. Therefore, no structural or non-structural application of the investigated WA materials has yet been validated based on the present results.

Further research is required before WA can be considered for practical implementation in cement-based products, particularly regarding long-term strength development, durability, dimensional stability, environmental performance, and application-specific requirements. Consequently, the main contribution of this study is the systematic comparison of different WA fractions and sequential treatment routes, providing guidance for future optimization and application-oriented research rather than direct validation of construction use.

4. Conclusions

This study evaluated the early-age mechanical performance of cement mortars incorporating wood ash (WA), including fly ash and bottom ash, as a 20% Portland cement replacement. The investigated WA was ball-milled prior to application, with additional treatments including water washing, slaking, calcination, and combined washing–calcination. The following key conclusions can be drawn:

- All mortars containing WA exhibited reduced compressive strength compared to the reference system, indicating limited early-age performance under the investigated conditions.
- The observed strength performance was comparable to that reported in some previous studies on biomass- and wood-ash-containing cement-based mortars, although higher strength or SAI values have also been reported under different material and treatment conditions.
- Wood bottom ash-based mixtures showed the best performance among all tested materials, with 28-day SAI values of approximately 65–71% obtained for ball-milled wood bottom ash (LBF_5, LBC_5, and Oz_5).
- For the wood fly ash, water-washing increased compressive strength and UPV while reducing water absorption, coinciding with reduced prominence of arcanite reflections in the XRD pattern of L_Fly_5_W.
- The XRD, UPV, water absorption, and compressive-strength results showed generally consistent trends among the investigated treatment conditions, although the present measurements do not establish direct causal relationships between these observations.
- The results of this study should be interpreted as early-age feasibility screening of WA in cement-based systems, while long-term strength development and durability performance remain outside the scope of this study.
- Further research should focus on extended curing periods to assess long-term performance, as well as more intensive mechanical activation, alternative thermal conditions, and chemical pre-treatment of WA to further enhance its performance in cement-based systems. In addition, durability-related investigations, including resistance to chloride ingress, freeze-thaw resistance, and alkali–silica reaction, are required to fully evaluate the long-term applicability of WA in cementitious materials.

Declaration of Generative AI usage

During the preparation of this work, the authors used ChatGPT to improve the readability and language of the manuscript. After using this tool, the authors reviewed and edited the content as needed and take full responsibility for the content of the published article.

Funding

This work has been supported by research and development grant No RTU-PA-2024/1-0012 under the EU Recovery and Resilience Facility funded project No. 5.2.1.1.i.0/2/24/I/CFLA/003 “Implementation of consolidation and management changes at Riga Technical University, Liepaja University, Rezekne Academy of Technology, Latvian Maritime Academy and Liepaja Maritime College for the progress towards excellence in higher education, science, and innovation”.

CRediT authorship contribution statement

Oskars Lescinskis: Writing – review & editing, Writing – original draft, Visualization, Validation, Software, Methodology, Investigation, Formal analysis, Data curation, Conceptualization. **Girts Bumanis:**

Writing – original draft, Validation, Resources, Methodology, Investigation, Formal analysis, Conceptualization. **Genadijs Sahmenko:** Writing – original draft, Validation, Resources, Methodology, Investigation. **Tatjana Tambovceva:** Validation, Supervision, Resources, Project administration, Funding acquisition. **Danute Vaiciukyniene:** Visualization, Validation, Methodology, Data curation. **Sakdirat Kaewunruen:** Writing – review & editing, Writing – original draft, Validation, Supervision, Methodology. **Diana Bajare:** Supervision, Resources, Project administration.

Declaration of competing interest

The authors declare that they have no known competing financial interests or personal relationships that could have appeared to influence the work reported in this paper.

Data availability

Data will be made available on request.

References

[1] F. Pomponi, A. Moncaster, Circular economy for the built environment: a research framework, J. Clean. Prod. 143 (2017) 710–718, https://doi.org/10.1016/j.jclepro.2016.12.055.

[2] N.Trong Lam, Assessment of the compressive strength and strength activity index of cement incorporating fly ash, IOP Conf. Ser.: Mater. Sci. Eng. 869 (2020) 032052, https://doi.org/10.1088/1757-899X/869/3/032052.

[3] R. Rumman, M.R. Kamal, A. Bediwy, M.S. Alam, Partially burnt wood fly ash characterization and its application in low-carbon mortar and concrete, Constr. Build. Mater. 402 (2023) 132946, https://doi.org/10.1016/j.conbuildmat.2023.132946.

[4] B.S. Thomas, J. Yang, K.H. Mo, J.A. Abdalla, R.A. Hawileh, E. Ariyachandra, Biomass ashes from agricultural wastes as supplementary cementitious materials or aggregate replacement in cement/geopolymer concrete: A comprehensive review, J. Build. Eng. 40 (2021) 102332, https://doi.org/10.1016/j.jobe.2021.102332.

[5] R.M. Andrew, Global CO2 emissions from cement production, 1928–2018, Earth Syst. Sci. Data 11 (2019) 1675–1710, https://doi.org/10.5194/essd-11-1675-2019.

[6] E.E. Teker Ercan, L. Andreas, A. Cwirzen, K. Habermehl-Cwirzen, Wood ash as sustainable alternative raw material for the production of concrete—a review, Materials 16 (2023), https://doi.org/10.3390/ma16072557.

[7] D. Ndahirwa, H. Zmamou, H. Lenormand, E. Chenot, S. Potel, N. Leblanc, Wood ash-based binders for lightweight building materials: Evaluating the influence of hydraulic lime and cement on the setting and mechanical properties of wood ash pastes, Results Eng 24 (2024) 102738, https://doi.org/10.1016/j.rineng.2024.102738.

[8] L.M. Ottosen, E.Ø. Hansen, P.E. Jensen, G.M. Kirkelund, P. Golterman, Wood ash used as partly sand and/or cement replacement in mortar, Int. J. Sustain. Dev. Plan. 11 (5) (2016) 781–791, https://doi.org/10.2495/SDP-V11-N5-781-791.

[9] S.V. Vassilev, C.G. Vassileva, Y.C. Song, W.Y. Li, J. Feng, Ash contents and ash-forming elements of biomass and their significance for solid biofuel combustion, Fuel 208 (2017) 377–409, https://doi.org/10.1016/j.fuel.2017.07.036.

[10] C. Belviso, State-of-the-art applications of fly ash from coal and biomass: a focus on zeolite synthesis processes and issues, Prog. Energy Combust. Sci. 65 (2018) 109–135, https://doi.org/10.1016/j.pecs.2017.10.004.

[11] M. Berra, T. Mangialardi, A.E. Paolini, Reuse of woody biomass fly ash in cement-based materials, Constr. Build. Mater. 76 (2015) 286–296, https://doi.org/10.1016/j.conbuildmat.2014.11.052.

[12] E.E. Teker Ercan, L. Andreas, A. Cwirzen, K. Habermehl-Cwirzen, Ground wood ash as a supplementary cementitious material: Effects on strength, durability and environmental performance of concrete, Constr. Build. Mater. 503 (2025) 144520, https://doi.org/10.1016/j.conbuildmat.2025.144520.

[13] X. Liang, H. Dong, Z. Li, C. Liu, S. Zhang, G. Ye, Characterization, pretreatment, and valorization of wood biomass fly ash in a binary cement-free binder, Developments in the Built Environment 23 (2025) 100700, https://doi.org/10.1016/j.dibe.2025.100700.

[14] Á.F. Do Couto, G.F.B. Sandoval, N. Schwantes-Cezario, A.R.F. Christoni, R.J. P. Cruz, P.R.C. da Silva, G. Morales, Physicochemical evaluation of Eucalyptus wood ash as a mineral admixture in Portland cement matrices: a preliminary study, Case Stud, Constr. Mater. 21 (2024) e03860, https://doi.org/10.1016/j.cscm.2024.e03860.

[15] M. Rosales, J. Rosales, F. Agrela, M.I. Sánchez de Rojas, M. Cabrera, Design of a new eco-hybrid cement for concrete pavement, made with processed mixed recycled aggregates and olive biomass bottom ash as supplementary cement materials, Constr. Build. Mater. 358 (2022) 129417, https://doi.org/10.1016/j.conbuildmat.2022.129417.

[16] I. Mehdipour, K.H. Khayat, Understanding the role of particle packing characteristics in rheo-physical properties of cementitious suspensions: a literature review, Constr. Build. Mater. 161 (2018) 340–353, https://doi.org/10.1016/j.conbuildmat.2017.11.147.

[17] F. Bülbül, L. Courard, Turning waste into greener cementitious building material: treatment methods for biomass ashes—a review, Materials 18 (2025), https://doi.org/10.3390/ma18040834.

[18] N.M. Sigvardsen, M.R. Geiker, L.M. Ottosen, Reaction mechanisms of wood ash for use as a partial cement replacement, Constr. Build. Mater. 286 (2021), https://doi.org/10.1016/j.conbuildmat.2021.122889.

[19] J.A. Olsson, S.A. Miller, J.D. Kneifel, A review of current practice for life cycle assessment of cement and concrete, Resour. Conserv. Recycl. 206 (2024), https://doi.org/10.1016/j.resconrec.2024.107619.

[20] T. Ramos, A.M. Matos, J. Sousa-Coutinho, Mortar with wood waste ash: mechanical strength carbonation resistance and ASR expansion, Constr. Build. Mater. 49 (2013) 343–351, https://doi.org/10.1016/j.conbuildmat.2013.08.026.

[21] O. Lescinskis, A. Sapata, G. Bumanis, M. Sinka, X. Zhou, D. Bajare, The potential of wood ash to be used as a supplementary cementitious material in cement mortars, Buildings 15 (2025), https://doi.org/10.3390/buildings15091507.

[22] LVS EN 933-1, A, Tests for Geometrical Properties of aggregates – Part 1: Determination of Particle Size Distribution – Sieving Method, CEN, Brussels, 2012, 2012.

[23] LVS EN 197-1, Cement – Part 1: Composition, Specifications and Conformity Criteria for Common Cements, CEN, Brussels, 2012, 2012.

[24] LVS EN 1015-3, Methods of Test for Mortar for Masonry – Part 3: Determination of Consistence of Fresh Mortar (by flow table), CEN, Brussels, 2000, 2000.

[25] K. Ohenoja, V. Wigren, J. Österbacka, M. Illikainen, Mechanically treated fly ash from fluidized bed combustion of peat, wood, and wastes in concrete, Waste Biomass Valor 11 (2020) 3071–3079, https://doi.org/10.1007/s12649-019-00615-y.

[26] E.E. Teker Ercan, R. Panek, M. Szeląg, A. Cwirzen, K. Habermehl-Cwirzen, The impact of the high-energy grinding of wood ash on its pozzolanic activity, Materials 18 (2025), https://doi.org/10.3390/ma18133100.

[27] L.C. Nascimento, et al., Use of wood bottom ash in cementitious materials: a review, J. Mater. Res. Technol. 23 (2023) 4226–4243, https://doi.org/10.1016/j.jmrt.2023.02.071.

[28] A.B. Ayobami, Performance of wood bottom ash in cement-based applications and comparison with other selected ashes: overview, Resour. Conserv. Recycl. 166 (2021), https://doi.org/10.1016/j.resconrec.2020.105351.

[29] Y. Barabanshchikov, K. Usanova, Influence of silica fume on high-calcium fly ash expansion during hydration, Materials 15 (2022), https://doi.org/10.3390/ma15103544.

[30] G.C.H. Doudart de la Grée, M.V.A. Florea, A. Keulen, H.J.H. Brouwers, Contaminated biomass fly ashes—characterization and treatment optimization for reuse as building materials, Waste Manage 49 (2016) 96–109, https://doi.org/10.1016/j.wasman.2015.12.023.

[31] X. Liang, Z. Li, H. Dong, G. Ye, A review on the characteristics of wood biomass fly ash and their influences on the valorization in cementitious materials, J. Build. Eng. (2024) 110927, https://doi.org/10.1016/j.jobe.2024.110927.

[32] ASTM C642, Standard Test Method for Density, Absorption, and Voids in Hardened Concrete, ASTM International, 2021, 2021.

[33] LVS EN 196-1, Methods of Testing Cement – Part 1: Determination of Strength, CEN, Brussels, 2016, 2016.

[34] X. Yao, et al., Characterization comparison of bottom ash and fly ash during gasification of agricultural residues, Fuel 285 (2021), https://doi.org/10.1016/j.fuel.2020.119122.

[35] Z. Lei, S. Pavia, Biomass ash waste as an activator to produce carbon-negative cement, Cement 18 (2024) 100112, https://doi.org/10.1016/j.cement.2024.100112.

[36] A. De Rossi, L. Simão, M.J. Ribeiro, D. Hotza, R.F.P.M. Moreira, Study of cure conditions effect on wood biomass fly ash geopolymers, J. Mater. Res. Technol. 9 (2020) 7518–7528, https://doi.org/10.1016/j.jmrt.2020.05.047.

[37] M. Czop, B. Łazniewska-Piekarczyk, Evaluation of leachability of fly ash and bottom ash from combustion of municipal waste, Sustainability 11 (2019) 9538, https://doi.org/10.3390/su11195384.

[38] R. Pöykiö, K. Manskinen, H. Nurmesniemi, O. Dahl, Comparison of trace elements in bottom ash and fly ash from a large-sized (77 MW) multi-fuel boiler at the power plant of a fluting board mill, Finland, Energy Explor. Exploit. 29 (3) (2011) 217–233, https://doi.org/10.1260/0144-5987.29.3.217.

[39] E. Fidanchevski, et al., Technical and radiological characterisation of fly ash and bottom ash, J. Radioanal. Nucl. Chem. 330 (2021) 685–694, https://doi.org/10.1007/s10967-021-07980-w.

[40] V.A. Vu, A. Cloutier, B. Bissonnette, P. Blanchet, J. Duchesne, Effect of wood ash as partial cement replacement in wood-cement panels, Materials 12 (2019), https://doi.org/10.3390/ma12172766.

[41] M.S. Rahman, M.E. Hossain, M.R. Islam, Environment-friendly alkaline solution for enhanced oil recovery, Pet. Sci. Technol. 26 (2008) 1596–1609, https://doi.org/10.1080/10916460701287557.

[42] J.Tiegoum Wembe, et al., Impact of partial substitution of cement and sand by ash from wood species, Discov. Civil Eng. 1 (2024), https://doi.org/10.1007/s44290-024-00035-5.

[43] J.T. Wembe, et al., Valorization of ashes from different wood species in cementitious materials, Discov. Sustain. 5 (2024), https://doi.org/10.1007/s43621-024-00460-7.

[44] I. Gabrijel, M.J. Rukavina, N. Štirmer, Influence of wood fly ash on concrete properties through filling effect mechanism, Materials 14 (2021) 7164, https://doi.org/10.3390/ma14237164.

[45] D. Nagrockienė, A. Daugėla, Investigation into the properties of concrete modified with biomass combustion fly ash, Constr. Build. Mater. 174 (2018) 369–375, https://doi.org/10.1016/j.conbuildmat.2018.04.125.
[46] J. Fořt, et al., Durability analysis of sustainable mortars with biomass fly ash, J. Build. Eng. 91 (2024), https://doi.org/10.1016/j.jobe.2024.109565.
[47] M. Chai, et al., Effects of thermal treatment on mortar with bottom ash replacing cement, J. Build. Eng. 100 (2025), https://doi.org/10.1016/j.jobe.2024.111742.
[48] N. Tripathi, C.D. Hills, R.S. Singh, S. Kyeremeh, A. Hurt, Mineralisation of CO_2 in wood biomass ash for cement substitution in construction products, Front. in Sustain. 5 (2024), https://doi.org/10.3389/frsus.2024.1287543.
[49] K.W. Kim, K.T. Park, F. Ates, H.G. Kim, B.H. Woo, Effect of pretreated biomass fly ash on cement mortar properties, Case Stud. Constr. Mater. 18 (2023), https://doi.org/10.1016/j.cscm.2022.e01754.
[50] K. Preethi, D. Ambika, S. Janani, A preliminary study on production of roof tiles and paver blocks using wood and coal ash, Mater, in: Today Proc., 2023, https://doi.org/10.1016/j.matpr.2023.01.124.
[51] S.A. Shah, M.A. Tantray, A.R. Bhat, Wood ash as an eco-friendly alternative for sustainable cement replacement in concrete, Clean. Circular Bioecon. 12 (2025) 100178, https://doi.org/10.1016/j.clcb.2025.100178.